



HAL
open science

Measurement of Thermal Conductivity and Thermal Resistance Through a Tiny Hot-Plate Experiment

Benjamin Rémy, Yves Jannot, A. Degiovanni

► **To cite this version:**

Benjamin Rémy, Yves Jannot, A. Degiovanni. Measurement of Thermal Conductivity and Thermal Resistance Through a Tiny Hot-Plate Experiment. *High Temperatures-High Pressures*, 2009, 39 (1), pp.11-31. hal-01971683

HAL Id: hal-01971683

<https://hal.univ-lorraine.fr/hal-01971683>

Submitted on 7 Jan 2019

HAL is a multi-disciplinary open access archive for the deposit and dissemination of scientific research documents, whether they are published or not. The documents may come from teaching and research institutions in France or abroad, or from public or private research centers.

L'archive ouverte pluridisciplinaire **HAL**, est destinée au dépôt et à la diffusion de documents scientifiques de niveau recherche, publiés ou non, émanant des établissements d'enseignement et de recherche français ou étrangers, des laboratoires publics ou privés.

Measurement of thermal conductivity and thermal resistance with a Tiny Hot Plate

Yves Jannot, Benjamin Rémy, Alain Degiovanni
LEMTA, Nancy-Université, CNRS,
2, avenue de la Forêt de Haye, BP 160 - 54504 VANDOEUVRE Cedex - France,

Abstract

A new thermal conductivity and thermal resistance measurement method is presented. This stationary method is dedicated to heterogeneous materials and systems to which transient measurement methods cannot be applied. The experimental device is detailed and an exact heat transfer model based on integral transforms is developed. The estimation method both with the uncertainty evaluation process is presented. Experimental results obtained with materials which thermal conductivities are known validate the method. An application to the measurement of the thermal resistance of a heterogeneous material (double glazing insert) is presented.

Keywords: measurement technique, thermal conductivity, stationary hot plate, quadrupolar model

NOMENCLATURE

e	Sample thickness	m
h	Lateral heat transfer coefficient	$W.K^{-1}.m^{-2}$
J_0	Bessel function of first kind and order 0	
J_1	Bessel function of first kind and order 1	
Nr	Norm of the integral transform	
M	Quadrupolar matrix	
P	Perimeter	m
R	Equivalent sample radius	m
r_c	Thermal contact resistance per surface unit	$m^2.K.W^{-1}$
r_{thm}	Measured thermal resistance per surface unit	$m.K.W^{-1}$
r_{thc}	Calculated thermal resistance per surface unit	$m.K.W^{-1}$
R_c	Thermal contact resistance	$K.W^{-1}$
R_e	Electric resistance	Ω
RC	Quadrupolar matrix of a contact resistance	
R_{th}	Thermal resistance	$K.W^{-1}$
S	Cross section	m^2
T	Temperature	$^{\circ}C$
U	Electric tension applied to the heating element	V
x	Space variable	m
z	Space variable	m
ϕ	Heat flux	W
λ	Thermal conductivity	$W.K^{-1}.m^{-1}$
θ	Temperature	$^{\circ}C$
$\bar{\theta}$	Mean temperature	$^{\circ}C$
θ_R	Lateral temperature	$^{\circ}C$
ω_n	Eigen values of the integral transform	

Subscripts

Cu	Cuivre
↑	Upper
↓	Lower

Introduction

Energy control requires to the development of more and more complex materials and systems which are difficult to characterize. It may concern thin thermal insulating materials for buildings, porous membranes for fuel cells or spacers for double-glazing. In all these applications concerning heterogeneous materials, classical transient techniques (flash method [1], hot wire [2], hot strip [3], or hot disc [4]) cannot be successfully used. This is particularly the case with materials for which it is not possible to define an equivalent homogeneous material and thus a thermal diffusivity. The guarded hot plate method [5] needs quite large samples that may be difficult to obtain for some specific materials. It is thus necessary to consider another approaches, less precise but allowing a thermal characterization for these types of materials.

Among these approaches, a Tiny Hot Plate device using a Peltier element as a fluxmeter is proposed. The development of this technique is based on the works performed by Batsale and Degiovanni [6]. An application for the measurement of the thermal resistance of spacers for double glazing will be presented.

1. Principle and experimental device

Figure 1 describes the principle of the experiment. The heating element is composed of a $39 \times 39 \times 0.16 \text{ mm}^3$ plane resistance inserted between two Kapton foils. Its electric resistance is $R = 40,5 \Omega$. All others elements exhibit a square geometry ($a = 40 \text{ mm}$).

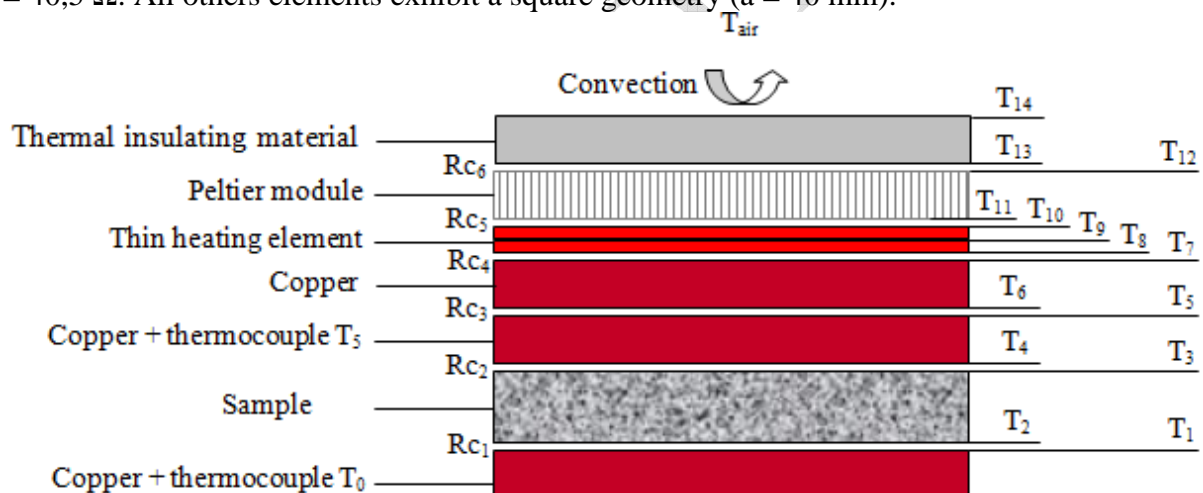


Figure 1 : Schema of the experimental device

Temperatures T_0 , T_5 and T_{air} are measured through K-type thermocouples with a 0.025 K resolution. Standard deviations in the temperature measurement can be reduced in steady-state regime by increasing the number of measurements. Tension applied through the heating element is measured with a 0.01 V accuracy. Contact resistances between the different elements are reduced using a thermoconductive grease and a loading system. The experimental device is presented in Figure 2

The principle of the experiment is to apply a tension U through the heating element to obtain $T_5 = T_{\text{air}}$. This allows us to get rid of the lateral heat losses in the two copper elements above the sample. The dissipated flux Φ_{\uparrow} on the upper part of the heating element is measured

through a Peltier element, which is used and calibrated as a fluxmeter. It allows an estimation of the value of the dissipated $\Phi_{9\downarrow}$ on its bottom face through the following relation:

$$\Phi_{9\downarrow} = \Phi_9 - \Phi_{9\uparrow} \quad (1)$$

With : $\phi_9 = \frac{U^2}{Re}$

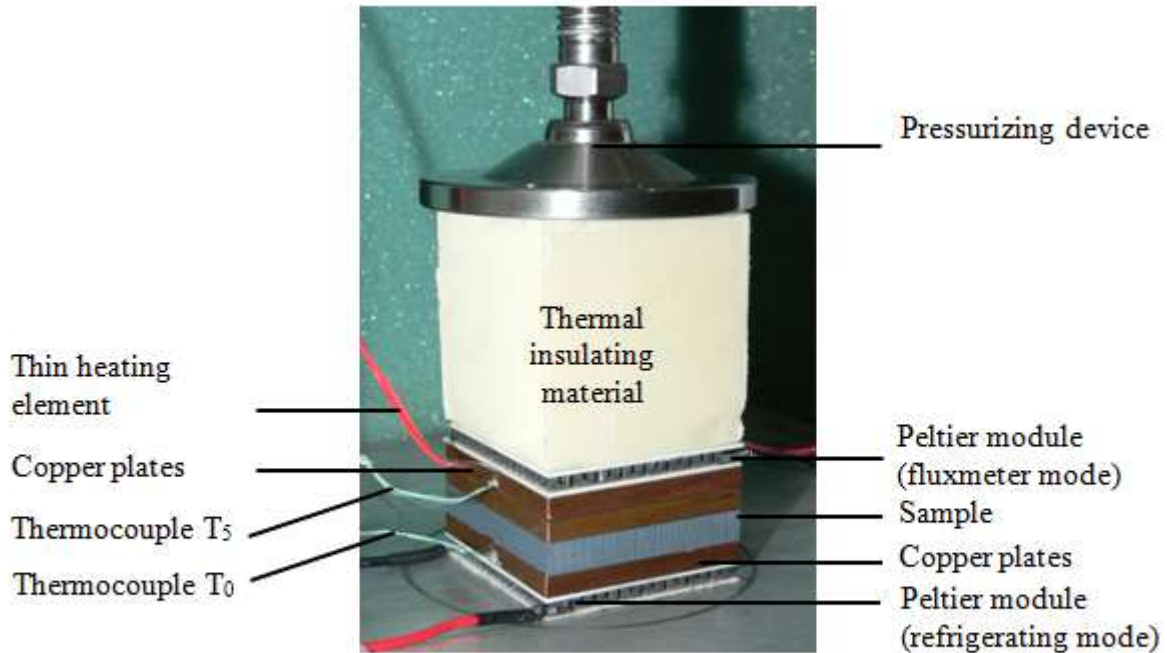


Figure 2 : View of the experimental device

Temperature T_0 is fixed through a thermostat or a Peltier element. This device measures the thermal resistance between the thermocouples T_0 and T_5 :

$$R_{th} = 2 R_{thCu} + 2 R_c + \frac{e}{\lambda S} \quad (2)$$

The measurement of the thermal conductivity is only possible in the case $\frac{e}{\lambda S} > 2 R_{thCu} + 2 R_c$ and is given by:

$$\lambda = \frac{e \phi_{9\downarrow}}{S (T_5 - T_0)} \quad (3)$$

The different contact resistances have been estimated by applying a tension of 10V through the heating element and by measuring the temperatures T_0 and T_5 without any sample. Considering $\lambda_{Copper} = 400 \text{ W.m}^{-1}.\text{K}^{-1}$, we obtain $r_c = 10^{-4} \text{ K.W}^{-1}.\text{m}^{-2}$. Thus, this method can be only applied for samples with $e > 0,01 \lambda$, in order to limit the errors caused by the contact resistance to a value lower than 2%. This limits the using of this method to low or middle conductivity materials (see § 4.2). Another method to get free of the contact resistances consists in making two measurements on the same material (1 and 2) with two different thicknesses:

$$R_{th1} = 2 R_{thCu} + 2 R_c + \frac{e_1}{\lambda S} \quad (4)$$

$$R_{th2} = 2 R_{thCu} + 2 R_c + \frac{e_2}{\lambda S} \quad (5)$$

It can be deduced:

$$\lambda = \frac{e_2 - e_1}{S (R_{th1} - R_{th2})} \quad (6)$$

Where: $R_{th2} = \left(\frac{T_5 - T_0}{\Phi_{9\downarrow}} \right)_2$ and $R_{th1} = \left(\frac{T_5 - T_0}{\Phi_{9\downarrow}} \right)_1$

This method is particularly interesting for thin samples (see § 4.2). Even though this condition is checked, the value given by relations (3) or (6) is affected by convective effects through the lateral faces of the sample that may affect the input or output fluxes through the sample, which are different from the $\Phi_{9\downarrow}$ value used for the estimation of λ . A modelling of the system taking into account these heat losses allows us to reduce the estimation errors.

2. Quadrupolar model

The system can be modelled through the quadrupole technique [7] by taking into account the lateral heat losses with a fin's model. The temperature in each stack element can be obtained by solving the following equation:

$$\frac{\partial^2 T}{\partial x^2} - \frac{h P}{\lambda S} (T - T_{air}) = 0 \quad (7)$$

Where:

- h global heat transfer coefficient
- P perimeter
- λ thermal conductivity
- S cross section

Front and Back faces temperatures of each element are linearly linked in the Laplace domain through the following quadrupole relation:

$$\begin{bmatrix} T_{i+1} - T_{air} \\ \phi_{i+1} \end{bmatrix} = \begin{bmatrix} A & B \\ C & D \end{bmatrix} \begin{bmatrix} T_i - T_{air} \\ \phi_i \end{bmatrix} \quad (8)$$

$$A = \text{ch}(\alpha e) = D$$

where : $B = \frac{1}{\lambda \alpha S} \text{sh}(\alpha e)$ with $\alpha^2 = \frac{h P}{\lambda S}$ and $e =$ element thickness

$$C = \lambda \alpha S \text{sh}(\alpha e)$$

The measured parameters are: T_0 , T_5 , ϕ_9 et $\phi_{9\uparrow}$.

Setting $\theta = T - T_{air}$, one can write (cf. electric schemes in figure 3) :

$$\begin{bmatrix} \theta_9 \\ \phi_{9\downarrow} \end{bmatrix} = [M5][RC4][M4][RC3][M3][RC2][M2][RC1][M1] \begin{bmatrix} \theta_0 \\ \phi_0 \end{bmatrix} = \begin{bmatrix} A_{90} & B_{90} \\ C_{90} & D_{90} \end{bmatrix} \begin{bmatrix} \theta_0 \\ \phi_0 \end{bmatrix} \quad (9)$$

and: $\begin{bmatrix} \theta_9 \\ \phi_{9\downarrow} \end{bmatrix} = [M5][RC4][M4][RC3] \begin{bmatrix} T_5 \\ \phi_5 \end{bmatrix} = \begin{bmatrix} A_{95} & B_{95} \\ C_{95} & D_{95} \end{bmatrix} \begin{bmatrix} \theta_5 \\ \phi_5 \end{bmatrix} \quad (10)$

The quadrupolar matrices correspond to the following elements:

- M1 Lower copper element maintained at T_0
- M2 Unknown sample
- M3 Copper element above the sample
- M4 Copper element under the sample
- M5 Half-thickness of the heating element (Kapton)

- RC1 Thermal contact resistance at M1/M2 contact
- RC2 Thermal contact resistance at M2/M3 contact
- RC3 Thermal contact resistance at M3/M4 contact
- RC4 Thermal contact resistance at M4/M5 contact

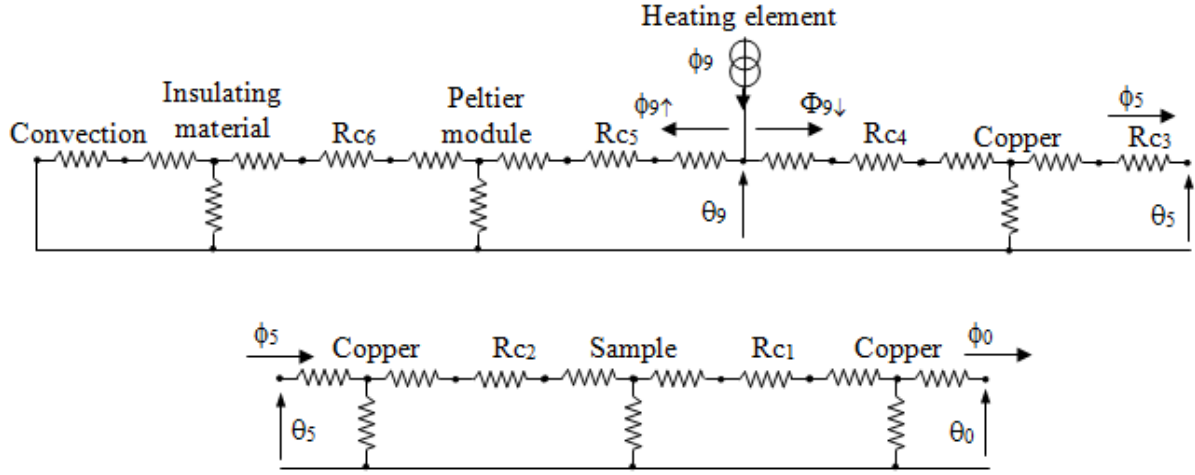


Figure 3 : Equivalent electrical diagram of the experimental device

It can be deduced from matrix relations (9) et (10):

$$D_{90} \theta_9 - B_{90} \phi_{9\downarrow} - (A_{90} D_{90} - B_{90} C_{90}) \theta_0 = 0 \quad (11)$$

$$D_{95} \theta_9 - B_{95} \phi_{9\downarrow} - (A_{95} D_{95} - B_{95} C_{95}) \theta_5 = 0 \quad (12)$$

θ_9 can be removed from these two equations to lead to the following equation where the only unknown quantities are the sample thermal conductivity λ , the heat transfer coefficient h and the copper-sample contact resistances. Indeed, $\Phi_{9\downarrow}$ is a known quantity that can be obtained from the flux $\Phi_{9\uparrow}$ given by the Peltier element (used as a fluxmeter) and the relation (1). If temperatures T_5 and a T_{air} are closed then the flux $\Phi_{9\uparrow}$ is always very low and the fluxmeter calibration has no significant influence on the measurement. $\Phi_{9\uparrow}$ appears as being a small corrective term compared to Φ_9 .

We finally obtain

$$D_{90} \frac{B_{95} \phi_{9\downarrow} - (A_{95} D_{95} - B_{95} C_{95}) \theta_5}{D_{95}} - B_{90} \phi_{9\downarrow} - (A_{90} D_{90} - B_{90} C_{90}) \theta_0 = 0 \quad (13)$$

The accuracy of λ obtained from this equation is better than the approximated value given by relation (3).

3. Validation of the lateral heat losses calculation by the fin model

In the proposed model, the fin's approximation is applied to take into account the lateral heat exchanges. Under this condition, no 3D resolution methods are required to solve the problem. Before validating this approximation, we will first show that it is an important point to take into account the lateral exchanges in the conductivity estimation.

3.1 Error caused by neglecting the lateral heat losses

To show the significant effect of the lateral exchanges in the thermal conductivity measurement, the lower part of the apparatus has been thermally simulated with the help of the software COMSOL (see Figure 4). To simplify the analysis, thermal contact resistances have been neglected. Table 1 give the characteristics of the whole stack elements. To neglect the contact resistances, thicknesses have been chosen with $e/\lambda > 0.01$.

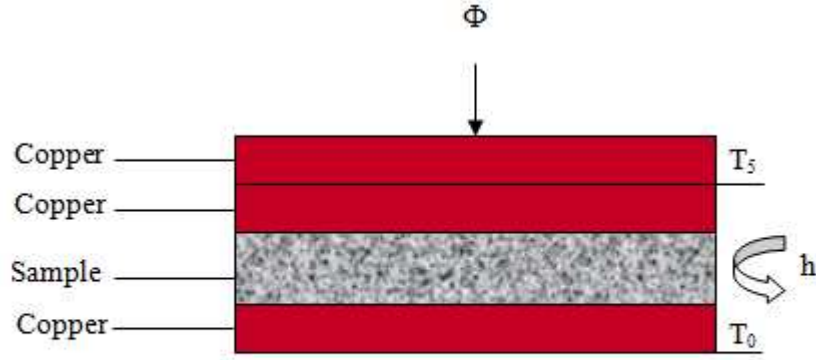


Figure 4 : Schema of the device simulated with FEMLAB

Table 1: Details of the simulated device

Material	Thermal conductivity (W.m ⁻¹ .K ⁻¹)	Thickness (mm)	Lateral dimensions (mm)
Copper	400	4	40 x 40
Sample	0.05 to 2.0	1 to 40	40 x 40

Temperature T_0 is fixed to $T_{\text{air}} - 5^\circ\text{C}$ and the heat flux value Φ is controlled so that $T_5 = T_{\text{air}}$. For different values of the heat reansfer coefficient h , the conductivity value λ has been calculated from the classical relation:

$$\lambda_{\text{estimated}} = \frac{e \phi}{S (T_5 - T_0)} \quad (14)$$

The results are represented in figure 5. We can notice that the lateral heat losses lead to an under-estimation of the thermal conductivity λ . The error, which can be larger than 10%, mainly depends on the ratio $\frac{h e^2}{\lambda}$.

This result can be easily explained. Indeed, the lateral heat flux $d\Phi_p$ at a given location z can be written as:

$$d\phi_p = h P [T_s(z) - T_{\text{air}}] dz \quad (15)$$

$T_s(z)$ being the surface temperature of the sample.

As a consequence, the temperature difference through a given element dz' at location z' is:

$$dT = \frac{dz'}{\lambda S} \left[\phi - \int_0^{z'} d\phi_p \right] \quad (16)$$

or for a sample with a thickness e :

$$\Delta T = \int_0^e \frac{dz'}{\lambda S} \left[\phi - \int_0^{z'} d\phi_p \right] \quad (17)$$

Assuming in first approximation $T_s(z)$ as being linear:

$$T_s(z) = \frac{T_0 - T_5}{e} z + T_5 \quad (18)$$

and taking into account the fact that $T_5 = T_{\text{air}}$, we find:

$$\Delta T = \frac{e \phi}{\lambda S} + \frac{h P e^2}{\lambda S 6} \Delta T \quad (19)$$

The imposed flux allowing to keep ΔT constant is:

$$\phi = \frac{\lambda S}{e} \Delta T \left(1 - \frac{h P e^2}{\lambda S 6} \right) \quad (20)$$

And consequently, relation (14) becomes: $\lambda_{\text{estimated}} = \lambda_{\text{real}} \left(1 - \frac{h P e^2}{\lambda S 6} \right)$ (21)

By taking into account the geometry of our stack ($P/S 100 \text{ m}^{-1}$):

$$\lambda_{\text{estimated}} = \lambda_{\text{real}} \left(1 - 16,7 \frac{h e^2}{\lambda} \right) \quad (22)$$

Figure 5 clearly shows that the approximating relation (22) is not precise enough for particular cases.

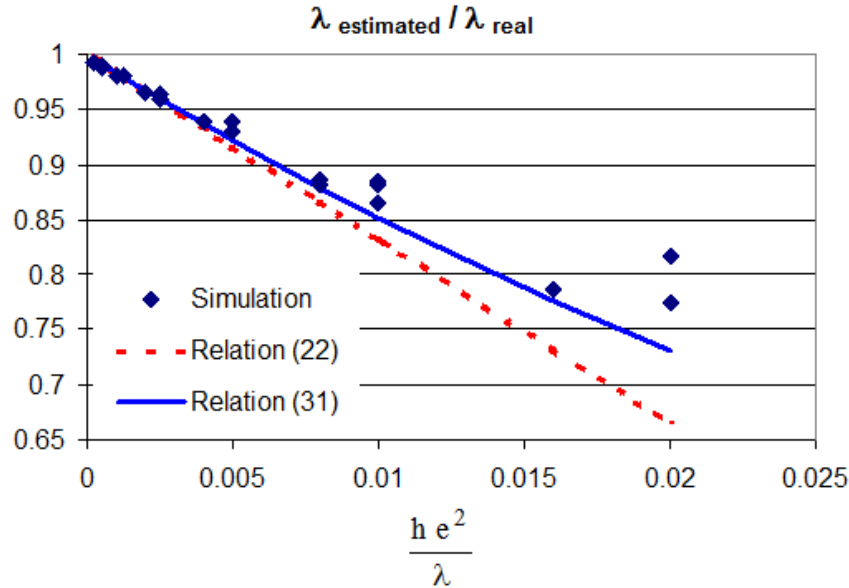


Figure 5 : Ratio of estimated and real values of the thermal conductivity

3.2 Fin's Model

For simplifying the calculations, an axial symmetry is assumed in our system. The square section can be viewed as a circular section by keeping the P/S ratio as constant and fixing the radius R of the circular section equal to a half-side $a/2$ of the square section. In that case, the axisymmetric 2D heat transfer equation is written:

$$\frac{1}{r} \frac{\partial}{\partial r} \left(r \frac{\partial T}{\partial r} \right) + \frac{\partial^2 T}{\partial z^2} = 0 \quad (23)$$

$$-\lambda \frac{\partial T}{\partial r} = h (T - T_{\text{air}}) \text{ if } r = R \quad (24)$$

$$\frac{\partial T}{\partial r} = 0 \text{ if } r = 0 \quad (25)$$

Let: $\theta = T - T_{\text{air}}$ and $\bar{\theta} = \frac{2}{R^2} \int_0^R T(r) r \, dr$

Integrating relation (23) over $[0, R]$ and using relations (24) and (25) yields:

$$\frac{d^2 \bar{\theta}}{dz^2} - \frac{2h}{\lambda R} \theta_R = 0 \quad (26)$$

θ_R being the surface temperature in $r = R$.

The classical fin's approximation consists in working the mean radial temperature $\theta_R = \bar{\theta}$:

$$\frac{d^2 \bar{\theta}}{dz^2} - \frac{2h}{\lambda R} \bar{\theta} = 0 \quad (27)$$

We find again the equation (7).

The solution of equation (27) (or (7)) can be represented (cf.[5]) by:

$$\begin{bmatrix} \bar{\theta}_0 \\ \phi_0 \end{bmatrix} = \begin{bmatrix} A & B \\ C & D \end{bmatrix} \begin{bmatrix} \bar{\theta}_e \\ \phi_e \end{bmatrix} \quad (28)$$

$\bar{\theta}_0$ and $\bar{\theta}_e$, Φ_0 and Φ_e represent the mean temperatures and heat fluxes in $z = 0$ and in $z = e$, respectively.

More particularly:
$$\phi_0 = \frac{D}{B} \bar{\theta}_0 - \frac{1}{B} \bar{\theta}_e \quad (29)$$

Applying this result to relation (14) :

$$\Phi \equiv \Phi_0$$

$$T_5 - T_0 = \bar{\theta}_0 - \bar{\theta}_e \text{ (temperature difference at the sample boundaries)}$$

with $T_5 = T_{\text{air}}$ so that: $\bar{\theta}_0 = 0$

and:
$$\lambda_{\text{estimated}} = \frac{e}{S} \left(-\frac{\bar{\theta}_e}{B} \right) / (-\bar{\theta}_e) \quad (30)$$

with $B = \frac{1}{\lambda \alpha S} \text{sh}(\alpha e)$ where $\alpha^2 = \frac{h P}{\lambda S}$

Finally:
$$\frac{\lambda_{\text{estimated}}}{\lambda_{\text{real}}} = \frac{\alpha e}{\text{sh}(\alpha e)} \quad (31)$$

After a second order asymptotic expansion of $\text{sh}(\alpha e)$, equation (31) exhibits the same form as equation (21), which thus appears to be a simplifying form of equation (31). Nevertheless, let notice that the relation (31) is only valid under the assumption $\theta_R = \bar{\theta}$. In particular, Figure 5 showed that this approximation is not always true in our facility.

3.3 Exact Solution through integral transforms

To obtain the exact solution of the set of equations (23), (24) and (25), integral transforms can

be used. In our case, the adapted integral transform is the Hankel transform with : $J_0\left(\omega_n \frac{r}{R}\right)$

being the eigenfunctions and ω_n the eigenfunctions defined as the roots of the following equation:

$$\omega_n J_1(\omega_n) = \text{Bi} J_0(\omega_n) \quad (32)$$

with J_0 and J_1 being the zeroth and first order Bessel functions of the first kind and $Bi = \frac{h R}{\lambda}$.

The integral transform is defined by: $\tilde{\theta} = \int_0^R r \theta J_0\left(\omega \frac{r}{R}\right) dr$ (33)

with the associated norm: $N_n = \int_0^R r \theta J_0^2\left(\omega_n \frac{r}{R}\right) dr = \frac{R^2}{2} [J_0^2(\omega_n) + J_1^2(\omega_n)]$ (34)

Applying the integral transform, equation (23) becomes:

$$\frac{d^2 \tilde{\theta}}{dz^2} - \frac{\omega_n^2}{R^2} \tilde{\theta} = 0 \quad (35)$$

(same form as the fin's equation)

The solution is given by: $\tilde{\theta}(\omega_n, z) = A \operatorname{ch}\left(\omega_n \frac{z}{R}\right) + B \operatorname{sh}\left(\omega_n \frac{z}{R}\right)$ (36)

with $\theta_0 = T_0 - T_{\text{air}}$ if $z = 0$

$\theta_e = T_e - T_{\text{air}}$ if $z = e$

so: $\tilde{\theta}_0 = \int_0^R \theta_0 r J_0\left(\omega_n \frac{r}{R}\right) dr = \theta_0 R^2 \frac{J_1(\omega_n)}{\omega_n}$ if $z = 0$ (37)

$\tilde{\theta}_e = \int_0^R \theta_e r J_0\left(\omega_n \frac{r}{R}\right) dr = \theta_e R^2 \frac{J_1(\omega_n)}{\omega_n}$ if $z = e$ (38)

Constants A and B can be determined from boundary conditions (37-38):

$$\tilde{\theta}(\omega_n, z) = R^2 \frac{J_1(\omega_n)}{\omega_n} \left[\left(\theta_e - \theta_0 \operatorname{ch}\left(\frac{\omega_n e}{R}\right) \right) \frac{\operatorname{sh}\left(\frac{\omega_n z}{R}\right)}{\operatorname{sh}\left(\frac{\omega_n e}{R}\right)} + \theta_0 \operatorname{ch}\left(\frac{\omega_n z}{R}\right) \right] \quad (39)$$

Finally, the solution is given by:

$$\theta(r, z) = \sum_n \frac{\tilde{\theta}(\omega_n, z) J_0\left(\frac{\omega_n r}{R}\right)}{N_n} \quad (40)$$

As the eigenvalues are function of the Biot number, they are different for each layer of the stack and require the computation of a large number of eigenvalues at each simulation for solving the heat transfer through the whole stack. The fin's approximation already gives quite satisfactory results. Thus, the idea in the following section will consist in using a simplifying solution to improve the classical fin's approximation.

3.4 Fin model correction

Equation (26) that can be also written as:

$$\frac{d^2 \bar{\theta}}{dz^2} - \frac{2 h}{\lambda R} \frac{\theta_R}{\bar{\theta}} \bar{\theta} = 0 \quad (41)$$

The classical fin's approximation yields: $\theta_R / \bar{\theta} = 1$

Let evaluate now the $\theta_R / \bar{\theta}$ ratio from the exact solution given by (40):

$$\bar{\theta}(z) = \sum_n \frac{\tilde{\theta}(\omega_n, z)}{N_n} \frac{2 J_1(\omega_n)}{\omega_n} \quad (42)$$

$$\theta_R(z) = \sum_n \frac{\tilde{\theta}(\omega_n, z)}{N_n} J_0(\omega_n) \quad (43)$$

In the more general case, the difficulty of this correction comes from the fact that it is a function of the z coordinate. To validate the proposed method, the $\theta_R/\bar{\theta}$ ratio will be calculated in $z = e/2$ by keeping either 6 terms or 100 terms in the series. Conversely, if we consider only the first term of the series, we find:

$$\frac{\theta_R}{\bar{\theta}} = \frac{\omega_0^2}{2 Bi} \quad (44)$$

The main interest of this correction is that it is very easy to implement in practice substituting $\frac{2 h}{\lambda R}$ by $\frac{\omega_0^2}{R^2}$ in the fin's equation, with ω_0 being the first root of equation (32). Another approximations have been also proposed by different authors (an expression better than 1% is proposed in Appendix I).

The estimated value of the thermal conductivity $\lambda_{\text{estimated}}$ can be then calculated from the relation:

$$\frac{\lambda_{\text{estimated}}}{\lambda_{\text{real}}} = \frac{\omega_0 e}{R \operatorname{sh}\left(\frac{\omega_0 e}{R}\right)} \quad (45)$$

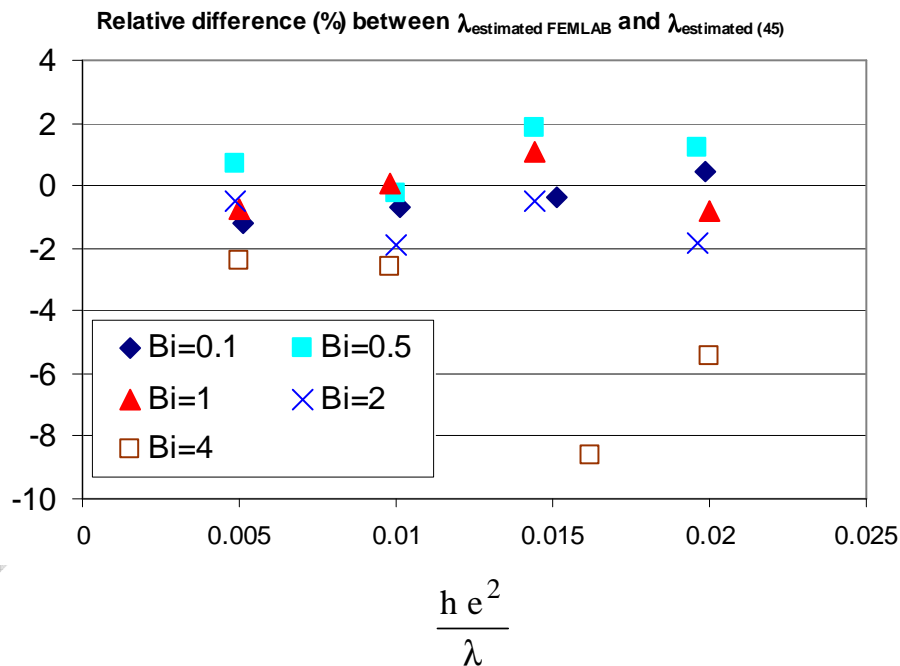


Figure 6 : Relative difference between the values of $\lambda_{\text{estimated}}$ obtained by simulation with FEMLAB and calculated with relation (45)

We can notice as shown in Figure 6 that for Biot numbers lower than or equal to 2, the values of the ratio $\lambda_{\text{estimated}}/\lambda_{\text{real}}$ calculated from relation (45) exhibit a difference lower than 2% compared to the values obtained from COMSOL computing results. More generally,

substituting $\frac{2h}{\lambda R}$ by $\frac{\omega_0^2}{R^2}$ in the fin's relation, this approximation is valid for large Biot values, up to 2 (compared to the classical approximation that is only valid for Biot numbers lower than 0.1).

3.5 Validation of the quadrupolar model with the corrected fin model

Table 2: Values of the thermal conductivity estimated with COMSOL and with the fin model considering different corrections.

h	W.m ⁻² .K ⁻¹	5	10	5	10
		$\lambda_{\text{real}} = 0,1 \text{ W.m}^{-1}.\text{K}^{-1}$ e = 1mm		$\lambda_{\text{real}} = 0,1 \text{ W.m}^{-1}.\text{K}^{-1}$ e = 5mm	
Φ_{COMSOL}	W.m ⁻²	498.1	497.0	98.0	96.4
$\lambda_{\text{without convection}}$	W.m ⁻² .K ⁻¹	0.0996	0.0995	0.0980	0.0965
λ_{fin}		0.0999	0.0999	0.1001	0.1005
$\lambda_{\text{fin corr. 1 term}}$		0.0999	0.0998	0.0997	0.0991
$\lambda_{\text{fin corr. 6 terms}}$		0.0999	0.0999	0.0999	0.1000
$\lambda_{\text{fin corr. 100 terms}}$		0.0999	0.0999	0.0999	0.1000
		$\lambda_{\text{real}} = 0.1 \text{ W.m}^{-1}.\text{K}^{-1}$ e = 10mm		$\lambda_{\text{real}} = 0.1 \text{ W.m}^{-1}.\text{K}^{-1}$ e = 20mm	
Φ_{COMSOL}	W.m ⁻²	46.53	44.07	19.32	16.44
$\lambda_{\text{without convection}}$	W.m ⁻² .K ⁻¹	0.0931	0.0882	0.0773	0.0654
λ_{fin}		0.1010	0.1031	0.1046	0.1123
$\lambda_{\text{fin corr. 1 term}}$		0.0993	0.0980	0.0995	0.0981
$\lambda_{\text{fin corr. 6 terms}}$		0.1000	0.1000	0.1004	0.1006
$\lambda_{\text{fin corr. 100 terms}}$		0.1000	0.1000	0.1004	0.1005
		$\lambda_{\text{real}} = 0.2 \text{ W.m}^{-1}.\text{K}^{-1}$ e = 4mm		$\lambda_{\text{real}} = 0.5 \text{ W.m}^{-1}.\text{K}^{-1}$ e = 10mm	
Φ_{COMSOL}	W.m ⁻²	248.0	246.5	245.6	241.9
$\lambda_{\text{without convection}}$	W.m ⁻² .K ⁻¹	0.1984	0.1972	0.4912	0.4838
λ_{fin}		0.1999	0.2000	0.4999	0.5006
$\lambda_{\text{fin corr. 1 term}}$		0.1998	0.1995	0.4995	0.4991
$\lambda_{\text{fin corr. 6 terms}}$		0.1999	0.1999	0.4997	0.4997
$\lambda_{\text{fin corr. 100 terms}}$		0.1999	0.1999	0.4998	0.4997
		$\lambda_{\text{real}} = 1 \text{ W.m}^{-1}.\text{K}^{-1}$ e = 20mm		$\lambda_{\text{real}} = 2 \text{ W.m}^{-1}.\text{K}^{-1}$ e = 40mm	
Φ_{COMSOL}	W.m ⁻²	241.6	243.3	233.9	219.9
$\lambda_{\text{without convection}}$	W.m ⁻² .K ⁻¹	0.9664	0.9372	1.8712	1.7592
λ_{fin}		1.0000	1.0020	2.007	2.0052
$\lambda_{\text{fin corr. 1 term}}$		0.9992	0.9990	1.9992	1.9997
$\lambda_{\text{fin corr. 6 terms}}$		0.9993	0.9995	1.9992	1.9998
$\lambda_{\text{fin corr. 100 terms}}$		0.9993	0.9995	1.9992	1.9998

To validate this method, the values of the imposed flux Φ determined by COMSOL and the temperature difference $T_5 - T_0 = 5 \text{ }^\circ\text{C}$ have been considered as experimental results. This data are then been used to estimate the conductivity λ by an inverse method based on the

quadrupole model taking into account the fin's effect. The estimated value are finally compared with the nominal values used in COMSOL simulations. The obtaining results for different values of the thermal conductivity λ , thickness e and heat transfer coefficient h are given in Table 2.

We can notice that the modified model using the first 6 terms of the series calculated with the approached function given in Appendix, allow us in all cases an estimation of the thermal conductivity λ better than 1% compared to its nominal value. The one term model is of course less precise but also very easy to use and gives quite satisfactory results (maximum error of about 2%). These results must be compared with those obtained by the classical fin's model that yields to large errors ($> 10\%$) in different cases.

4. Estimation errors on the thermal conductivity

In practice, it is difficult to precisely evaluate the heat transfer coefficient h and the contact resistances R_c between the sample and copper elements. In the next sections, we are going to give an estimation of the uncertainties caused by these ill-known parameters.

4.1 Experiment with a single sample

The assumption of a convective heat transfer coefficient included between 5 and $10 \text{ W.m}^{-2} \cdot \text{K}^{-1}$ and contact resistances R_c between $5 \cdot 10^{-5} \text{ m}^2 \cdot \text{K.W}^{-1}$ and $2 \cdot 10^{-4} \text{ m}^2 \cdot \text{K.W}^{-1}$ is made.

Through the quadrupole model taking into account the lateral heat losses (100 terms), tension required to obtain $T_5 = T_{\text{air}}$ is calculated for each configuration and the two following "extreme" conditions:

1. $h = 10 \text{ W.m}^{-2} \cdot \text{K}^{-1}$ et $rc = 2 \cdot 10^{-4} \text{ m}^2 \cdot \text{K.W}^{-1}$
2. $h = 5 \text{ W.m}^{-2} \cdot \text{K}^{-1}$ et $rc = 5 \cdot 10^{-5} \text{ m}^2 \cdot \text{K.W}^{-1}$

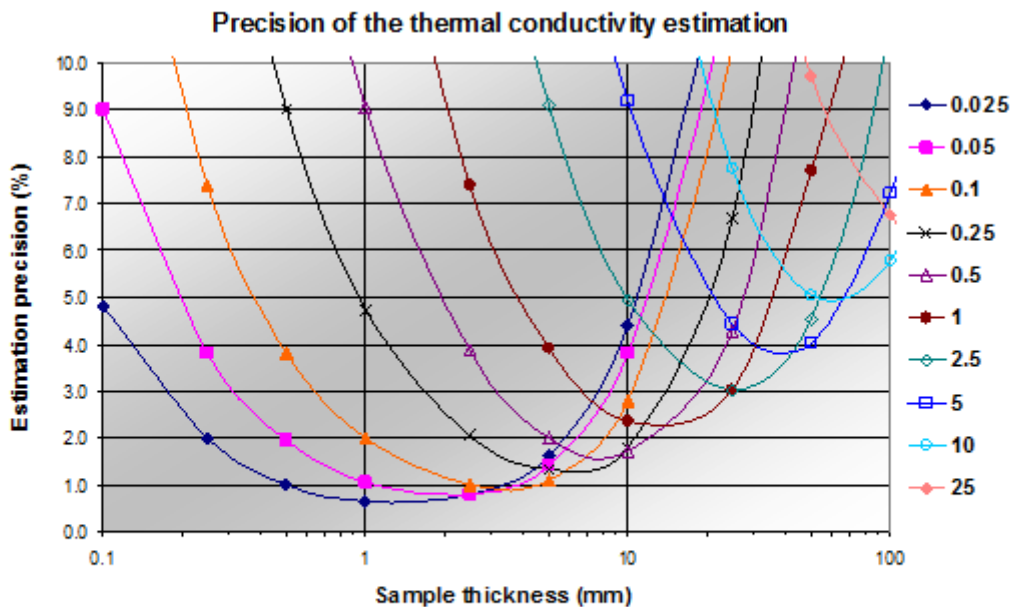


Figure 7 : Precision (%) of the estimation of the thermal conductivity as a function of the sample thickness (mm)

We perform for each values two estimations of λ (λ_1 and λ_2) by an inverse method based on the quadrupole model (relation (13)) with a correction of the lateral heat losses (6 terms) and using a fixed (mean) values for $h = 7.5 \text{ W.m}^{-2} \cdot \text{K}^{-1}$ and $rc = 10^{-4} \text{ m}^2 \cdot \text{K.W}^{-1}$. The error on the

estimated value of λ caused by uncertainties on h and rc is then defined from the two differences $|\lambda - \lambda_1|$ et $|\lambda - \lambda_2|$. The corresponding results are represented in the figure 7.

4.2 Precision improvement with two samples of different thickness

It is possible to get rid of the uncertainties on h or rc by making two experiments with two different thicknesses samples. The 3 unknown parameters λ , h and rc are obtained using relation (13) (in the single sample experiment, h and rc values are fixed to mean nominal values in the estimation of λ).

* Case of conducting materials ($\lambda > 2 \text{ W.m}^{-1}.\text{K}^{-1}$)

In this case, errors introduced by contact resistance and the heat transfer coefficient (h value between $5\text{-}10 \text{ W.m}^{-2}.\text{K}^{-1}$) has no effect on the estimation (see Table 2). The h value is then fixed to a mean value ($h = 7.5 \text{ W.m}^{-2}.\text{K}^{-1}$) and λ and rc are estimated by an inverse method from relation (13) written for each measurement.

* Case of insulating materials ($e/\lambda > 0.1 \text{ m}^2.\text{K.W}^{-1}$)

In this case, contact resistance errors can be neglected (lower than 1%) and rc is fixed to a mean value ($rc = 10^{-4} \text{ m}^2.\text{K.W}^{-1}$). λ and h are estimated by an inverse method from two equations given by relation (13) written for each experiment.

* Simulation results

For a conducting material with $\lambda = 10 \text{ W.m}^{-1}.\text{K}^{-1}$, $h = 10 \text{ W.m}^{-2}.\text{K}^{-1}$ and $rc = 2.10^{-4} \text{ m}^2.\text{K.W}^{-1}$ and for two different thicknesses $e_1 = 1 \text{ cm}$ and $e_2 = 2 \text{ cm}$. The results obtained from each simulation (setting $h = 7.5 \text{ W.m}^{-2}.\text{K}^{-1}$ and $rc = 10^{-4} \text{ m}^2.\text{K.W}^{-1}$) are $\lambda_1 = 8.33 \text{ W.m}^{-1}.\text{K}^{-1}$ and $\lambda_2 = 9.07 \text{ W.m}^{-1}.\text{K}^{-1}$. Using the two experiments simultaneously and setting $h = 7.5 \text{ W.m}^{-2}.\text{K}^{-1}$, we obtain: $\lambda_{12} = 9.91 \text{ W.m}^{-1}.\text{K}^{-1}$ and $rc = 1.96 \text{ m}^2.\text{K.W}^{-1}$.

For an insulating material with $\lambda = 0.025 \text{ W.m}^{-1}.\text{K}^{-1}$, $h = 5 \text{ W.m}^{-2}.\text{K}^{-1}$ and $rc = 2.10^{-4} \text{ m}^2.\text{K.W}^{-1}$ and for two different thicknesses $e_1 = 2 \text{ cm}$ and $e_2 = 5 \text{ cm}$. The results obtained for each independent experiment (setting $h = 7.5 \text{ W.m}^{-2}.\text{K}^{-1}$ and $rc = 10^{-4} \text{ m}^2.\text{K.W}^{-1}$) are $\lambda_1 = 0.0272 \text{ W.m}^{-1}.\text{K}^{-1}$ and $\lambda_2 = 0.0298 \text{ W.m}^{-1}.\text{K}^{-1}$ respectively. Using the two experiments simultaneously and setting $rc = 10^{-4} \text{ m}^2.\text{K.W}^{-1}$, we obtain: $\lambda_{12} = 0.0250 \text{ W.m}^{-1}.\text{K}^{-1}$ and $h = 5.00 \text{ W.m}^{-2}.\text{K}^{-1}$.

4.3 Experimental results

Using relation (13), λ_1 has been estimated setting $h = 5 \text{ W.m}^{-2}.\text{K}^{-1}$, $rc = 5.10^{-5} \text{ m}^2.\text{K.W}^{-1}$ and λ_2 has been obtained setting $h = 10 \text{ W.m}^{-2}.\text{K}^{-1}$, $rc = 2.10^{-4} \text{ m}^2.\text{K.W}^{-1}$.

Glass Sample:

Experiment 1: $e = 5.92 \text{ mm}$: $\lambda_1 = 1.013 \text{ W.m}^{-1}.\text{K}^{-1}$

$\lambda_2 = 1.075 \text{ W.m}^{-1}.\text{K}^{-1}$

Experiment 2: $e = 2.07 \text{ mm}$: $\lambda_1 = 1.008 \text{ W.m}^{-1}.\text{K}^{-1}$

$\lambda_2 = 1.185 \text{ W.m}^{-1}.\text{K}^{-1}$

Experiment 1 + Experiment 2: $\lambda = 1.015 \text{ W.m}^{-1}.\text{K}^{-1}$, $rc = 5.01.10^{-5} \text{ m}^2.\text{K.W}^{-1}$

The result does not depend on h for values included in the range

$$5 \text{ W.m}^{-2}.\text{K}^{-1} < h < 10 \text{ W.m}^{-2}.\text{K}^{-1}.$$

An independant measurement obtained from a differential calorimeter and a flash experiment gives:

$a = 5.00.10^{-7} \text{ m}^2.\text{s}^{-1}$, $\rho c = 2.00.10^6 \text{ J.kg}^{-1}$ leading to: $\lambda = 1.00 \text{ W.m}^{-1}.\text{K}^{-1}$

The difference between the two results is about of 1,5%.

Titanium Sample:

$e = 3.10 \text{ mm}$: $\lambda_1 = 4.84 \text{ W.m}^{-1}.\text{K}^{-1}$

$$\lambda_2 = 9.15 \text{ W.m}^{-1}.\text{K}^{-1}$$

The Hot-disk and Hot plane probe lead to the following value: $\lambda = 6.60 \text{ W.m}^{-1}.\text{K}^{-1}$

High density Polyethylene Sample:

$$e = 7.88 \text{ mm} : \quad \lambda_1 = 0.396 \text{ W.m}^{-1}.\text{K}^{-1}$$

$$\lambda_2 = 0.407 \text{ W.m}^{-1}.\text{K}^{-1}$$

The manufacturer value is: $\lambda = 0.42 \text{ W.m}^{-1}.\text{K}^{-1}$

Expanded Polystyrene sample with 38 kg.m^{-3} density:

$$e = 18.00 \text{ mm} : \quad \lambda_1 = 0.0334 \text{ W.m}^{-1}.\text{K}^{-1}$$

$$\lambda_2 = 0.0367 \text{ W.m}^{-1}.\text{K}^{-1}$$

PVC Sample:

$$e = 5.88 \text{ mm} : \lambda_1 = 0.1808 \text{ W.m}^{-1}.\text{K}^{-1}$$

$$\lambda_2 = 0.1858 \text{ W.m}^{-1}.\text{K}^{-1}$$

4.4 Double glass window spacers

Working in a steady-state regime allows us to measure the thermal resistances of heterogeneous materials. An example is given by the thermal characterization of double glass window spacers (see Figure 8).



Figure 8 : View of the characterized spacers

To perform this measurement, the spacers have been split into six 40 mm long pieces gathered to obtain a 40 mm x 40 mm sample with thicknesses included between 15 and 20 mm (air layer thickness of the double glass). Table 3 gives the spacers properties and the thermal resistance by unit length (r_{thm} in m.K.W^{-1}).

Table 3: Spacers characteristics

	Sample1	Sample 2	Sample 3
Layer 1	Aluminium e = 0.3 mm	Plastics e = 1 mm	Plastics e = 1 mm
Layer 2	Air E = 6 mm	Air E = 4.45 mm	Air e = 5 mm
Layer 3	Aluminium e = 0.3 mm	Plastics e = 1 mm	Plastics e = 1 mm
Layer 4		Aluminium e = 0.04 mm	Steel (inox) e = 0.1 mm
$r_{\text{thm}} (\text{m.K.W}^{-1})$	0.126	2.32	6.37
$r_{\text{thc}} (\text{m.K.W}^{-1})$	0.129	2.01	7.12

For comparison, a theoretical value (r_{thc} in $m.K.W^{-1}$) obtained from a parallel model is given. As properties of each layer (λ and e) are badly known (see Table 4), this last value must be considered as a simple order of magnitude.

Table 4: Thermal conductivity of the layers

Material	Aluminium	Air	Plastics	Steel (inox)
λ ($W.m^{-1}.K^{-1}$)	200	0.025	0.3	20

Conclusion

A simple and easy to use apparatus allowing the measurement of the thermal conductivity of insulators or low conductivity materials (thermal conductivity included between 0.025 down to 5 $W.m^{-1}.K^{-1}$) as well as the thermal resistance of heterogeneous systems (from 2.10^{-1} to $10^{-3} m^2.K.W^{-1}$) has been presented. The main interest of this facility stays in its ability to perform measurement on sample with small dimensions (40 mm x 40 mm width and 1 to 30 mm height). A precise and theoretical study has been carried out on the effects of the lateral heat losses (heat transfer coefficient h) and thermal contact resistance r_c and allowed us to set up an optimal estimation procedure taking into account their effects. The theoretical model proposed in this study is based on the fin's approximation but has been extended in the cases of large Biot number (>2), which allows us to keep the quadrupole approach and to develop a accurate and simple estimation procedure. Nevertheless, when the sample is available with a single thickness, it is not possible to get totally free from h and r_c parameters (the thermal conductivity being correlated to heat losses and contact resistances). We have given in this study the resulting uncertainties versus the thermal conductivity and the thickness of the sample. In the case of double thicknesses samples, it is possible to get almost totally free from h and r_c values by making two different experiments on two different thicknesses samples. Finally, different experimental results have been presented.

Appendix 1

Approximate relations for the roots of the equation $\beta J_1(\beta) = Bi J_0(\beta)$

$$\beta_i^2(Bi) = \beta_i^2(Bi = 0) + \frac{a_{1i} Bi + (\beta_i^2(Bi = \infty) - \beta_i^2(Bi = 0)) Bi^2}{b_{1i} + b_{2i} Bi + Bi^2} \quad (1)$$

Table 1: Coefficients in relation (1) for the first six roots.

i	1	2	3	4	5	6
$\beta_i(Bi = 0)$	0	3.8317	7.0156	10.1735	13.3237	16.4706
$\beta_i(Bi = \infty)$	2.4048	5.5201	8.6537	11.7915	14.9309	18.0711
a_{1i}	18.3237	52.7206	135.9384	273.2410	429.5111	639.8128
b_{1i}	9.1714	26.8437	70.0034	140.0121	223.1145	332.8289
b_{2i}	5.1080	7.1083	10.9044	15.0738	18.6848	22.5854
Maximum deviation (%) 0.01 < Bi < 100	0.069	0.021	0.027	0.028	0.020	0.016

Appendix 2

Relation between U_{Peltier} and $(T_5 - T_{\text{air}})$

In practice, it is difficult to precisely measure the temperature T_{air} in a location where convection is weak (low heat transfer coefficient between air and thermocouple) and where radiation takes place between one side of the thermocouple and walls submitted to large temperature gradients and in the other side with a cooling surface. A more precise estimation of T_{air} can be obtained through the measurement of the tension of the Peltier element.

$$\phi_9 = \phi_{9\downarrow} + \phi_{9\uparrow}$$

$$\phi_{9\downarrow} = \frac{T_9 - T_5}{R_{ec} + R_{Cu} + 2 R_{\text{contact}}} = \frac{T_9 - T_5}{R_{95}}$$

$$\phi_{9\uparrow} = \frac{T_9 - T_{\text{air}}}{R_{ec} + R_{\text{Peltier}} + R_{\text{insulation}} + R_{\text{convection}} + 2 R_{\text{contact}}} = \frac{T_9 - T_{\text{air}}}{R_{9a}}$$

$$\phi_{9\uparrow} = \frac{T_{11} - T_{12}}{R_{\text{Peltier}}}$$

$$\phi_9 = \frac{T_9 - T_5}{R_{95}} + \frac{T_9 - T_{\text{air}}}{R_{9a}} \quad T_9 = \frac{\phi_9 + \frac{T_5}{R_{95}} + \frac{T_{\text{air}}}{R_{9a}}}{\frac{1}{R_{95}} + \frac{1}{R_{9a}}}$$

$$T_{11} - T_{12} = \phi_{9\uparrow} R_{\text{Peltier}} = R_{\text{Peltier}} \frac{R_{95} \phi_9 + T_5 - T_{\text{air}}}{R_{9a} + R_{95}}$$

$$\text{So: } \phi_{\text{Peltier}} = \frac{U_{\text{Peltier}}}{k} = \frac{T_{11} - T_{12}}{R_{\text{Peltier}}} \quad \text{and:} \quad U_{\text{Peltier}} = k \frac{R_{95} \phi_9 + T_5 - T_{\text{air}}}{R_{9a} + R_{95}} ;$$

$$T_5 - T_{\text{air}} = (R_{9a} + R_{95}) \frac{U_{\text{Peltier}}}{k} - R_{95} \phi_9$$

Application in our facility:

Heating element: two Kapton layers, thickness 0.075mm ($\lambda \approx 0.2 \text{ W.m}^{-1}.\text{K}^{-1}$)

Insulating material: Polyurethan foam, thickness 2 cm ($\lambda \approx 0.04 \text{ W.m}^{-1}.\text{K}^{-1}$)

$k = 0.155 \text{ mV.m}^2.\text{W}^{-1}$; $R_{\text{contact}} = 10^{-4} \text{ m}^2.\text{K}.\text{W}^{-1}$

$$r_{9a} = \frac{0.000075}{0.2} + \frac{0.004}{1} + \frac{0.02}{0.04} + \frac{0.004}{400} + 0.0002 + \frac{1}{5} = 0.705 \text{ m}^2.\text{K}.\text{W}^{-1}$$

so: $R_{9a} = 440 \text{ K}.\text{W}^{-1}$

$$r_{95} = \frac{0.000075}{0.2} + \frac{0.004}{400} + 0.0001 = 0.000485 \text{ m}^2.\text{K}.\text{W}^{-1} \quad \text{if } r_c = 5.10^{-5} \text{ m}^2.\text{K}.\text{W}^{-1}$$

$$r_{95} = \frac{0.000075}{0.2} + \frac{0.004}{400} + 0.0004 = 0.000785 \text{ m}^2.\text{K}.\text{W}^{-1} \quad \text{if } r_c = 2.10^{-4} \text{ m}^2.\text{K}.\text{W}^{-1}$$

The mean value is: $R_{95} = 0,397 \text{ K}.\text{W}^{-1}$

After calculation, to obtain $T_5 - T_a = 0^\circ\text{C}$, $U_{\text{Peltier}} = 0.0873 \Phi_9$ must be imposed.

Example:

Considering: $\phi = 0.1 \text{ W}$, we must take: $U_{\text{Peltier}} = 0.0873 \phi = 0.00873 \text{ mV}$

If $R_{\text{contact}} = 5.10^{-5} \text{ m}^2.\text{K}.\text{W}^{-1}$, $T_5 - T_{\text{air}} = 0.027\text{K}$

If $R_{\text{contact}} = 2.10^{-4} \text{ m}^2.\text{K}.\text{W}^{-1}$, $T_5 - T_{\text{air}} = 0.036\text{K}$

The error on the difference $T_5 - T_{\text{air}}$ is less than 0.036K that is more precise than a direct measurement of the temperature in a motionless air.

REFERENCES

1. Matteis P., Campagnoli E., Firrao D., Ruscica G., Thermal diffusivity measurements of metastable austenite during continuous cooling, International Journal of thermal Sciences, 2007.
2. Franco A., An apparatus for the routine measurement of thermal conductivity of materials for building application based on a transient hot-wire method, Applied Thermal Engineering, vol.27, pp. 2495-2504, 2007.
3. Jannot Y., Meukam P., Simplified estimation method for the determination of thermal effusivity and thermal conductivity with a low cost hot strip, Measurement Science and Technology, vol.15, pp. 1932-1938, 2004.
4. Gustafsson S.E., Transient plane source techniques for thermal conductivity and thermal diffusivity measurements of solids materials, Rev. Sci. Instrum., 62, 3, pp. 797-804 1991.
5. Zhou W., Qi S., An Q., Zhao H., Liu N., Thermal conductivity of boron nitride reinforced polyethylene composites, Materials Research Bulletin, vol.42, pp. 1863-1873, 2007.
6. Batsale J.-C., Mesure de résistance thermique de plaques minces à l'aide d'une mini-plaque chaude, Revue Générale de Thermique, n° 390-391, pp. 387-391, 1994.
7. Maillet D., Andre S., Batsale J.-C., Degiovanni A., Moyne C., Thermal quadrupoles, Wiley, New York, 2000.